

Spectroscopic characterization of 78 DENIS ultracool dwarf candidates in the solar neighborhood and the Upper Sco OB association

E. L. Martín^{1,2} N. Phan-Bao,^{3,4} M. Bessell,⁵ X. Delfosse,⁶ T. Forveille,⁶ A. Magazzù,⁷ C. Reylé,⁸ H. Bouy,¹ R. Tata²

¹ Instituto de Astrofísica de Canarias, C/ Vía Láctea s/n, E-38200 La Laguna (Tenerife), Spain
e-mail: ege@iac.es

² University of Central Florida, Dept. of Physics, PO Box 162385, Orlando, FL 32816-2385, USA
e-mail: tata@physics.ucf.edu

³ Department of Physics, HCMIU, Vietnam National University Administrative Building, Block 6, Linh Trung Ward, Thu Duc District, HCM, Vietnam
e-mail: pbngoc@hcmiu.edu.vn

⁴ Institute of Astronomy and Astrophysics, Academia Sinica, PO Box 23-141, Taipei 106, Taiwan
e-mail: pbngoc@asiaa.sinica.edu.tw

⁵ Research School of Astronomy and Astrophysics, College of Science, Australian National University, ACT 2611, Australia
e-mail: bessell@mso.anu.edu.au

⁶ Laboratoire d'Astrophysique de Grenoble, Université J. Fourier, BP 53, 38041 Grenoble, France
e-mail: [forveille,delfosse]@obs.ujf-grenoble.fr

⁷ Telescopio Nazionale Galileo, Rambla José Ana Fernández Pérez 7 E-38712 Breña Baja, Spain
e-mail: magazzu@tng.iac.es

⁸ Observatoire de Besançon, Institut UTINAM, University of Franche-Comté, CNRS-UMR 6213, BP 1615, 25010 Besançon Cedex, France
e-mail: celine@obs-besancon.fr

Received ; accepted

ABSTRACT

Aims. Report Low-resolution optical spectroscopic observations for 78 very low-mass star and brown dwarf candidates that have been photometrically selected using the DENIS survey point source catalogue.

Methods. Spectral types are derived for them using measurements of the PC3 index. They range from M6 to L4. H α emission and NaI subordinate doublet (818.3 nm and 819.9 nm) equivalent widths are measured in the spectra. Spectroscopic indices of TiO, VO, CrH and FeH molecular features are also reported.

Results. A rule-of-thumb criterion to select young very low-mass objects using the NaI doublet equivalent width is given. It is used to confirm seven new members of the Upper Sco OB association and two new members of the R Cr-A star-forming region. Four of our field objects are also classified as very young, but are not members of any known nearby young association. The frequency of lower-gravity young objects in our field ultracool sample is 8.5%. Our results provide the first spectroscopic classification for 38 ultracool dwarfs in the solar vicinity with spectrophotometric distances in the range 17 pc to 65 pc (3 of them are new L dwarfs within 20 pc).

Key words. stars: low mass, brown dwarfs — solar neighborhood — stars: distances.

1. Introduction

A complete census of the solar neighborhood is needed for many different purposes. To mention just a few examples: the understanding of the star formation history of the Milky Way; the identification of bright benchmark objects of different spectral types and evolutionary history, and the search for extrasolar planets. Henry et al. (2002) estimated that more than half of the stellar systems within 25 pc are still unknown, and most of them are thought to be ultracool dwarfs (UDs; defined as those with spectral types M6–M9, L and T; Martín et al. 1996, 1997, 1999; Kirkpatrick et al. 1999, 2000), which include a mixture of very low-mass stars and substellar-mass brown dwarfs. Indeed, many UD candidates within 25 pc have been found in the last few years (Phan-Bao et al. 2008; Reid et al. 2008).

Large optical/infrared surveys have made a significant impact in the identification of our coolest neighbours. The Deep Near Infrared Survey of the Southern Sky (DENIS; Epchtein et al. 1997) has enabled the discovery of many UD candidates in the solar vicinity (Delfosse et al. 1997, 2001; Crifo et al. 2005; Phan-Bao et al. 2001, 2003, 2008; Kendall et al. 2004) and prompted the development of a new spectral class, the L dwarfs (Martín et al. 1997, 1999; Delfosse et al. 1999), which is characterized by the condensation of dust grains in the atmospheres (Allard et al. 2001; Marley et al. 2002; Tsuji 2005).

The Sloan Digital Sky Survey (SDSS; York et al. 2000) and the Two Micron All Sky Survey (2MASS; Skrutskie et al. 1997) have also brought about the discoveries of many UD candidates (Kirkpatrick et al. 1999, 2000; Fan et al. 2000; Knapp et al. 2004, Cruz et al. 2007, Reid et al. 2008) and have provided the identification of the coolest spectral class, the T dwarfs, character-

Send offprint requests to: N. Phan-Bao

ized by the presence of methane bands in the near-infrared spectrum (Burgasser et al. 2006; Kirkpatrick 2005). The new generation large infrared surveys CFHTLS and UKIDSS are starting to identify even cooler dwarfs (Warren et al. 2007), the so-called Y class, for which the distinguishing characteristic may be the emergence of ammonia molecular bands in the near infrared. Two objects with possible ammonia absorption have recently been identified (Delorme et al. 2008), but their classification as Y dwarfs remains controversial because they are very similar to late T dwarfs (Burningham et al. 2008).

The characterization of the nearby ultracool population continues to be a goal of recent papers. Besides those mentioned above, it is worthwhile to mention a few more. Kendall et al. (2007) presented twenty-one southern ultracool dwarfs (M7–L5.5) selected from 2MASS and SuperCOSMOS point source databases according to their colors and proper motions, and confirmed via low-resolution near-infrared spectroscopy. Costa et al. (2006) and Henry et al. (2006) reported trigonometric parallaxes for several UD, including the closest known L dwarf. Jameson et al. (2008) have provided proper motion measurements for over a hundred L and T dwarfs.

In this paper we present low-resolution optical spectra of 78 UD candidates selected from the DENIS point source catalog using photometric color criteria. For a subsample of them (50 objects with galactic latitude between 30 and 15 degrees), the Maximum Reduced Proper Motion (MRPM) method (Phan-Bao et al. 2003, 2008) is used to reject giants. We also present spectra of a few DENIS UD candidates in the general area of the Upper Sco OB associations.

2. SAMPLE SELECTION AND SPECTROSCOPIC OBSERVATIONS

Most (71 out of 78) of our sample comes from a systematic search of 10,000 square degrees of the DENIS database (available at the Paris Data Analysis Center, PDAC) for potential UD members of the solar neighbourhood that are redder than $I - J \geq 3.0$ and have galactic latitudes $|b_{ll}| \geq 15^\circ$ (Delfosse et al. 2003). 21 of them have galactic latitudes $|b_{ll}| > 30$, and the other 50 were extracted from a selection with a galactic latitude criterion less restricting ($|b_{ll}| > 15$) and for which the MRPM method was used to discriminate nearby ultracool dwarfs from distant red giants (Phan-Bao et al. 2003, 2008). Proper motions were measured using Aladin and the Digital Sky Survey¹ (DSS). They will be given in another paper that will deal with the analysis of the kinematics of the UDs. 7 of our targets come from a search for low-mass members of the Upper Sco OB association (Martín, Delfosse & Guieu 2004). We covered 60 square degrees looking for objects redder than $I - J \geq 2.3$. The names, coordinates and photometry of all targets are provided in Table 1.

Spectroscopy of DENIS candidates presented herein was obtained in several observing runs using different telescopes. Following a chronological order, we started on March 2000 with ALFOSC on the Nordic Optical Telescope in La Palma. The grism number 5 provided a dispersion of 3.1 Å per pixel. Our second observing run was in September 2000 with the red arm of the ISIS spectrograph mounted on the 4.2-m William Herschel telescope in La Palma. The grating R158R provided a dispersion of 2.9 Å per pixel. The same telescope and instrumental configuration were again used on December 2006. However, a different

CCD was installed, resulting in a dispersion of 1.6 Å per pixel. A slit of 1 arcsec gave a spectral resolution of 6.5 Å.

On December 2000 and November 2003, we used the ESO NTT with the EMMI instrument in its Red Imaging and Low-Dispersion mode (RILD). In this mode the dispersion is 2.8 Å pixel⁻¹, and the effective wavelength range is 520 to 950 nm. The spectrophotometric standards, LTT 2415 and Feige 110 were chosen from the ESO list. All reduction was performed within MIDAS. We selected the 1" slit, which corresponds to a spectral resolution of 10.4 Å.

Spectroscopic data of more DENIS candidates were collected on August 2002 with the FORS2 spectrograph mounted on the 8-m Very Large Telescope in Paranal. The grating 600I provided a dispersion of 1.3 Å per pixel. Additional DENIS objects were observed at the 2.3-m telescope of the Sidings Springs Observatory (SSO) in Australia between 22 and 28 June 2006. The Double Beam Spectrograph with gratings 158R and 316R was used providing dispersions of 3.7 Å, and 1.87 Å respectively. The last observing run included in this paper took place on 17 July 2007 at the Blanco 4-m telescope in the Cerro Tololo Interamerican Observatory (CTIO). The spectroscopic observing log that summarizes all these observations is provided in Table 2.

All the spectra were reduced following standard procedures within the IRAF environment (bias and flatfield correction, wavelength calibration using a CuNeAr lamp, and flux calibration using standards), except the SSO spectra which were reduced in the FIGARO environment.

3. Spectral Types

Low-resolution CCD spectra have been used to define the spectral classification of late-M and early-L dwarfs (Kirkpatrick et al. 1999; Martín et al. 1996, 1999). The PC3 index defined by the latter authors has been used in several papers to determine spectral types (Crifo et al. 2005; Martín et al. 2004, 2006; Phan-Bao & Bessell 2006, 2008; Reylé et al. 2006). Comparisons with other methods of spectral type determination have found that the results are consistent. We have measured the PC3 index in our spectra, and we have determined spectral subclasses following the relationships given by Martín et al. (1999). The results are given in Table 3.

We obtained spectra for seven UDs in common with Martín et al. (1999). The spectral types obtained from measurement of the PC3 index in our spectra are in very good agreement with their values. Therefore the spectral classification adopted in this paper is tied to that of Martín et al. (1999), which is consistent within one spectral subclass with that of Kirkpatrick et al. (1999) for dwarfs earlier than L4. All the spectral types were checked by visual inspection and compared to standards from Martín et al. (1999). Full spectra of some of the latest type objects in our sample are shown in Figure 1.

We found that 34 of our targets already had spectral types in the literature (see references in the caption to Table 3). The largest overlap of objects with spectral types estimated independently is with Reid et al. (2008). In Figure 2, we show the comparison between our spectral types and those in the literature. Generally, there is a fairly good agreement; most of the dwarfs have the same spectral type within ± 1 subclass. We find spectral subclasses consistent with Reid et al. 2008 within 1 spectral subclass for all the 12 UDs in common.

For 5 objects we obtain spectral subclasses that deviate by more than 1 subclass with respect to those published in other pa-

¹ http://archive.stsci.edu/cgi-bin/dss_plate_finder

pers. Three of them, namely DENIS J0314352–462341, DENIS J0301488–590302 and DENIS J1216121–125731 had spectral types estimated from $I - J$ colors (Bouy et al. 2003). Our spectral type determination supersedes theirs, and underscores the limitations of using color-spectral class relations for ultracool dwarfs. The other two objects are DENIS J0357290–441731 and DENIS J1004283–114648. Both of them are binaries, and therefore our spectra are composites of 2 components of different spectral class. The spectral types of the resolved components given by Martín et al. (2006) should be more accurate than ours.

4. Surface gravity

Spectroscopic surface gravity estimates have been used to identify giants and young brown dwarfs among samples of ultracool candidates (Martín et al. 1996; Luhman et al. 1998; Gorlova et al. 2003; Martín & Zapatero Osorio 2003; McGovern et al. 2004; Allers et al. 2006). Atomic gravity-sensitive features present in our spectra include the KI resonance doublet at 766.5 nm and 766.9 nm, and the NaI subordinate doublet at 818.3 nm and 819.9 nm. We have used the NaI doublet because it is located in a region of stronger pseudocontinuum emission and it is less affected by telluric lines than the KI doublet. The measured equivalent widths of the NaI doublet are given in Table 4. Due to the low spectral resolution of most of our spectra, we chose to measure the combined equivalent width of the two lines.

Figure 3 illustrates the dependence between NaI equivalent widths and spectral class in our sample. There is a lot of scatter in the figure and no clear trend between NaI and spectral class. Part of this spread in equivalent widths could be due to the different instruments used in this work and to measurement uncertainties. For example, VB10 was observed at SSO with a spectral resolution of 8.5 Å, and at CTIO with a spectral resolution of 7.5 Å. The two spectra are overplotted in Figure 4. Note that the NaI doublet appears to be wider in the lower resolution spectrum because of blending effects with other absorption features. To measure consistent equivalent widths in spectra of different resolutions we established as a rule that the pseudo-continuum region was between 823 nm and 827 nm, and we integrated the line from 817.5 nm to 821.0 nm. The measurements were done manually with the IRAF task `splot`, and the exact integrations limits and continuum levels were judged individually for each spectrum, keeping the rule as a general guideline, but modifying it slightly as required by the shape of the observed spectrum. For our two spectra of VB10, we derived equivalent widths of 7.3 ± 0.6 Å, and 6.2 ± 0.3 Å, respectively. The lower value corresponds to the higher resolution spectrum. We conclude that the difference in equivalent width due to observing the same object with different instruments can be larger than the uncertainty in the equivalent width measurement.

From Figure 3, we infer that the objects with the weakest NaI are likely to have low surface gravity. As a rule of thumb we can state that *any object of spectral class between M6 and L4, and with a NaI (818.3, 819.9 nm) doublet detectable but weaker than field counterparts observed with the same spectral resolution, is likely to have a low surface gravity and consequently a very young age (younger than the Pleiades cluster, i.e. 100 Myr) and a substellar mass.* Note that the equivalent width determination may depend on the spectral resolution of the observations, and thus it is important to compare the young UD candidates with objects observed with similar spectral resolution.

As shown in Figure 3, all of the 7 targets in the Upper Sco OB association (solid hexagons) have weak NaI as expected for

young brown dwarfs. Putting this result together with the 28 very low-mass objects confirmed by Martín et al. 2004, brings the total number of DENIS discovered Upper Sco members to 35.

Two of our candidates have relatively early M type and no detectable NaI doublet. They are classified as giants in Table 4. Such a low contamination by giants is consistent with previous results and it is expected because the faint magnitudes of our candidates would place them (if they were giants) at distances over 300 parsecs from the Galactic disk.

The following field objects have weak NaI, indicative of lower surface gravity: DENIS-P J0141582–463358 (L0), which was suggested to be a young brown dwarf or planetary mass object by Kirkpatrick et al. (2006); DENIS-P J0006579–643654 (L0); DENIS-P J0443373+000205 (M9.5); DENIS-P J1703356–771520 (M9); DENIS-P J1901391–370017 (M8) and DENIS-P J1935560–284634 (M9.5). Figures 5 and 6 show comparisons of the spectra of some of these objects compared with dwarfs of the same spectral class observed with the same instrumental setup. In addition to the weak NaI doublet, the lower-gravity objects also have stronger VO bands and weaker FeH bands than their higher-gravity counterparts. Figure 7 illustrates this effect; the low-gravity objects display higher values of the VO/FeH molecular band ratio than the rest of the dwarfs in our sample. Figure 8 displays the full spectra of five of our low-gravity field objects, and of one of our Upper Sco BDs.

DENIS-P J1901391–370017 is located in the region of the Corona Australis (R-CrA) molecular cloud complex. There are 29 young objects listed in SIMBAD in an area of 2 arcmin around the DENIS source position, and one infrared source at only 3 arcsec. In fact the infrared source reported by Wilking et al. (1997) is the same as DENIS-P J1901391–370017 because the apparent magnitudes are consistent. The DENIS object has a low surface gravity and M8 spectral type, and it could be the second brown dwarf discovered with DENIS in the R-CrA star-forming region after DENIS-P J1859509–370632 (Bouy et al. 2004). On the other hand, DENIS-P J1935560–284634 (M9.5) is near this region, and could also be related to the R-CrA star-formation region. This object could be the third substellar-mass member detected by DENIS in this region and it deserves further attention.

DENIS-P J0006579–643654; DENIS-P J0443373+000205 and DENIS-P J1703356–771520 appear to be examples of a very young isolated brown dwarf or planetary-mass object that are not obviously associated with any known star-forming region. However, we note that DENIS J0608528–275358, which was identified by Cruz et al. (2003) as a young object because of enhanced VO absorption, does not have a remarkable weak NaI doublet, and thus its young brown dwarf status remains unconfirmed.

A subset of our targets have already been recognized as high proper motion objects. DENIS-P J0031192–384035; DENIS-P J0050244–153818; DENIS-P J0227102–162446; DENIS-P J0921141–210445; DENIS-P J1019245–270717; were previously known to be high proper motion objects (Deacon, Hambly & Cooke 2005). They are listed in Simbad with the names of 2MASS J00311925–3840356 or SIPSJ0031–3840; 2MASS J00502444–1538184 or SIPS J0050–1538; 2MASS J02271036–1624479 or SIPS J0227–1624; 2MASS J09211410–2104446 or SIPS J0921–2104; 2MASS J10192447–2707171 or SIPS J1019–2707, respectively. We confirm all of them as higher-gravity old nearby UDs on the basis of their strong NaI doublet and late spectral type. Their spectrophotometric distances, together with those of all

other old UDs in our sample, are given in Table 5. We used our adopted spectral types, the photometry given in Table 1 and the absolute J-band magnitude estimated from the absolute magnitude vs. $I - J$ color relationship given in Phan-Bao et al. (2008). This relationship is not valid for young BDs, and thus we do not give spectrophotometric distances from them.

The fraction of young BDs identified in our field sample (not including Upper Sco) is 6/71 (8.5%). Further work to observe these young BDs with higher spectral resolution is needed in order to detect lithium, an indicator of youth and substellar mass for UDs (Magazzù et al. 1993), and to compare with theoretical models in order to derive surface gravities.

5. A search for dusty disks in young BD candidates

We searched the *Spitzer* archive for complementary mid-IR data of our young BD candidates. Three targets (DENIS-P J0141582–463358, J1611296–190029 and J1901391–370017) have been observed with IRAC and MIPS. Table 6 gives the details of the observations. We retrieved the pipeline processed images and extracted the photometry using standard PSF photometry routines within the Interactive Data Language (IDL). Table 7 shows the photometry of the three sources. DENIS-P J1611296–190029 and J1901391–370017 do not have any counterpart in the MIPS1 image. We derive upper limits by adding a scaled PSF at the expected position of the target until the $3\text{-}\sigma$ detection algorithm finds it. Uncertainties, including instrumental, calibration and measurement errors, are estimated to add up to 10%. Figure 8 shows the spectral energy distribution of the three young BDs with *Spitzer* data. **Comparison with known dwarfs of similar spectral class does not reveal any significant infrared excess in the three objects as seen in young M dwarfs (e.g., Young et al. 2004) and BDs (e.g., Riaz et al. 2006). We therefore conclude that there is no evidence for dusty disks in these young BD candidates with our current data.**

6. Chromospheric activity

$H\alpha$ emission equivalent widths have been determined in our spectra using the line integration option in the *splot* IRAF task. Error bars were assessed object by object by repeated measurements using visual judgement of the continuum level and the line integration limits. The equivalent width values or upper limits are given in Table 4.

Gizis et al. (2000) reported low-resolution optical spectra for 53 M7–M9 dwarfs and 7 L dwarfs selected from the 2MASS survey. They found that all of their M7–M8 dwarfs displayed $H\alpha$ emission, but the frequency of $H\alpha$ emitters dropped abruptly for cooler dwarfs. Similar results were reported by West et al. (2004) in spectroscopic follow-up of a large photometrically selected sample from the SDSS. In a sample of 152 late-M and L dwarfs, Schmidt et al. (2007) found a slightly lower frequency of $H\alpha$ emitters among the M8 dwarfs and confirmed the decline of $H\alpha$ emission in L dwarfs. Our data indicates a frequency of $H\alpha$ emitters that is consistent with that of Schmidt et al. (2007) in the range M8–M9, but it drops faster in the L dwarfs. We do not attach high significance to our results because it is possible that our lower fraction of $H\alpha$ emitters in the L dwarfs is due to the low spectral resolution and modest signal-to-noise ratio of our spectra. For example, we observed DENIS J1004283–114648 with the NOT and the VLT (Table 2). $H\alpha$ emission is detected only in the VLT spectrum, which has a resolution 10 times better than the NOT spectrum.

In Figure 10, we show the dependence of $H\alpha$ emission equivalent width with respect to spectral class in our sample. The upper envelope of chromospheric $H\alpha$ emission given by Barrado y Navascués & Martín (2003) is shown as a dotted line. Only one object lies above this threshold and thus it is a strong candidate to harbour an active accretion disk. This object belongs to the Upper Sco sample. Our finding of 1 accretor among 7 members in Upper Sco is consistent with the fraction of accretors (5/28) reported by Martín et al. (2004) using the same criterion.

All of our 7 objects in Upper Sco and 4 out of 6 of our field lower-gravity objects have detected $H\alpha$ emission. The frequency $H\alpha$ emitters is higher among the very young objects than for the rest of our sample, but $H\alpha$ emission is not observed in all young VLM objects. As a rule of thumb we can state that *$H\alpha$ emission may be an indicator of youth, but its detection is not required for an object with a spectral class between M6 and L4 to be classified as young.*

We did not detect any obvious flares in our observations. Schmidt et al. (2007) estimated a flare cycle of 5% for late-M dwarfs and of 2% for L dwarfs. Those numbers may need to be revised slightly downwards. We plan to make a comprehensive study of the flare statistics in UDs in a future paper.

7. Candidate wide binaries

Using Simbad, we checked for objects within 2 arcminutes of our targets. DENIS J0000286–124514 has an X-ray source named 1RXS J000025.0–124519. No additional information is available on this X-ray source, so it is not possible to assess the probability that the DENIS source and the X-ray source are related.

DENIS J1115297–242934 has a star named TYC 6653-245-1 with $B=11.7$ and $V=11.1$. The proper motion of this star is -83.7 and 41.3 mas yr $^{-1}$ in RA and Dec., respectively. According to the NOMAD catalog the proper motion of DENIS J1115297–242934 is 14.0 and -138.0 mas yr $^{-1}$ in RA and Dec., respectively. Hence, the proper motions of the two sources are not consistent with a physical connection.

Acknowledgements. E.L.M. acknowledges financial support from NSF grant AST 0440520 and Spanish MEC grant AYA 2007-67458. N.P.-B. has been aided in this work by a Henri Chretien International Research Grant administered by the American Astronomical Society. X.D. and T.F. acknowledge financial support from the "Programme National de Physique Stellaire" (PNPS) of CNRS/INSU, France. We thank the referee, John Gizis, for his useful comments on our manuscript. DENIS is the result of a joint effort involving human and financial contributions of several Institutes mostly located in Europe. It has been supported financially mainly by the French Institut National des Sciences de l'Univers, CNRS, and French Education Ministry, the European Southern Observatory, the State of Baden-Wuerttemberg, and the European Commission under networks of the SCIENCE and Human Capital and Mobility programs, the Landessternwarte, Heidelberg and Institut d'Astrophysique de Paris.

References

- Allard, F., Hauschildt, P., Alexander, D., Tamanai, A., & Schweitzer, A. 2001, *ApJ*, 556, 357
- Allers, K. N., Kesser-Silacci, J. E., Cieza, L. A., & Jaffe, D. T. 2006, *ApJ*, 644, 364
- Barrado y Navascués, D. & Martín, E. L. 2003, *AJ*, 126, 2997
- Bouy, H., Brandner, W., Martín, E. L., Delfosse, X., Allard, F., & Basri, G. 2003, *AJ*, 126, 1526
- Bouy, H., et al. 2004, *A&A*, 424, 213
- Burgasser, A. J., Geballe, T. R., Leggett, S. K., Kirkpatrick, J. D., & Golimowski, D. A. 2006, *ApJ*, 637, 1067
- Burningham, B., et al. 2008, *MNRAS*, submitted (arXiv e-print 0806.0067)
- Costa, E., Méndez, R. A., Jao, W.-C., Henry, T. J., Subasavage, J.P., & Ianna, P. A. 2006, *AJ*, 132, 123

- Crifo, F., et al. 2005, *A&A*, 441, 653
- Cruz, K. L., et al. 2003, *AJ*, 126, 2421
- Cruz, K. L., et al. 2007, *AJ*, 133, 439
- Deacon, N.R., Hambly, N. C. & Cooke, J. A. 2005, *A&A*, 435, 363
- Delfosse, X., et al. 1997, *A&A*, 327, L25
- Delfosse, X., Tinney, C. G., Forveille, T., Epchtein, N., Borsenberger, J., Fouqué, P., Kimenswenger, S., & Tiphéne, D. 1999, *A&AS*, 135, 41
- Delfosse, X., et al. 2001, *A&A*, 366, L13
- Delfosse, X., Martín, E. L., Guieu, S., Forveille, T., Borsenberger, J., Epchtein, N., Fouque, P., & Simon, G. 2003, *SF2A*, p. 585
- Delorme, P., et al. 2008, *A&A*, 482, 961
- Epchtein, N. 1997, in *The Impact of Large Scale Near-IR Sky Surveys*. Kluwer Academic, Dordrecht, ed. Garzon F. et al., 15
- Fan, X., et al. 2000, *AJ*, 119, 928
- Gizis, J. E., Monet, D., Reid, I. N., Kirkpatrick, J. D., Liebert, J., & Williams, R. J. 2000, *AJ*, 120, 1085
- Gorlova, N. I., Meyer, M. R., Rieke, G. H., & Liebert, J. 2003, *ApJ*, 593, 1074
- Jameson, R. F., Casewell, S. L., Bannister, N. P., Lodieu, N., Keresztes, K., Dobbie, P. D., & Hodgkin, S. T. 2008, *MNRAS*, 384, 1399
- Hawley, S. L., et al. 2002, *AJ*, 123, 3409
- Henry, T. J., Walcovicz, L. M., Barto, T. C., & Golimowski, D. A., 2002, *AJ*, 123, 2002
- Henry, T. J., Wei-Chun, J., Subasavage, J. P., et al. 2006, *AJ*, 132, 2360
- Kendall, T. R., Maun, N., Azzopardi, M., & Gigoyan, K. 2003, *A&A*, 403, 929
- Kendall, T. R., Delfosse, X., Martín, E. L., & Forveille, T. 2004, *A&A*, 416, L17
- Kendall, T. R., Jones, H. R. A., Pinfield, D. J., Pokorny, R. S., Folkes, S., Weights, D., Jenkins, J. S., & Maun, N. 2007, *MNRAS*, 374, 445
- Kirkpatrick, J. D., Reid, I. N., Liebert, J., et al. 1999, *ApJ*, 519, 802
- Kirkpatrick, J. D., et al. 2000, *AJ*, 120, 447
- Kirkpatrick, J. D., et al. 2006, *ApJ*, 639, 1120
- Kirkpatrick, J. D. 2005, *ARAA*, 43, 195
- Knapp, G. R., et al. 2004, *AJ*, 127, 3553
- Luhman, K. L., Rieke, G. H., Lada, C. J., & Lada, E. A. 1998, *ApJ*, 508, 347
- Magazzù, A., Martín, E. L., & Rebolo, R. 1993, *ApJ*, 404, L17
- Marley, M. S., Seager, S., Saumon, D., Lodders, K., Ackerman, A. S., Freedman, R. S., & Fan, X. 2002, *ApJ*, 568, 335
- Martín, E. L., Rebolo, R., & Zapatero Osorio, M. R. 1996, *ApJ*, 469, 706
- Martín, E. L., Basri, G., Delfosse, X., & Forveille, T. 1997, *A&A*, 327, L29
- Martín, E. L., Delfosse, X., Basri, G., Goldman, B., Forveille, T., & Zapatero Osorio, M. R. 1999, *AJ*, 118, 2466
- Martín, E. L., & Zapatero Osorio, M. R. 2003, *ApJ*, 593, L113
- Martín, E. L., Delfosse, X., & Guieu, S. 2004, *AJ*, 127, 449
- Martín, E. L., Brandner, W., Bouy, H., Basri, G., Davis, J., Deshpande, R., & Montgomery, M.M. 2006, *A&A*, 456, 253
- McGovern, M. R., Kirkpatrick, J. D., McLean, I. S., Burgasser, A., Prato, L., & Lowrance, P. J. 2004, *ApJ*, 600, 1020
- Phan-Bao, N., Guibert, J., Crifo, F., Delfosse, X., Forveille, T., et al. 2001, *A&A*, 380, 590
- Phan-Bao, N., Crifo, F., Delfosse, X., Forveille, T., Guibert, J., et al. 2003, *A&A*, 401, 959
- Phan-Bao, N., & Bessell, M. S. 2006, *A&A*, 446, 515
- Phan-Bao, N., Bessell, M.S., Martín, E. L., Simon, G., et al. 2008, *MNRAS*, 383, 831
- Riaz, B., Gizis, J. E., & Hmiel, A. 2006, *ApJ*, 639, L79
- Reid, I. N., et al. 2006, *AJ*, 132, 891
- Reylé, C., Scholz, R. D., Schultheis, M., Robin, A. C., & Irwin, M. 2006, *MNRAS*, 373, 705
- Schmidt, S. J., Cruz, K. L., Bongiorno, B. J., Liebert, J., & Reid, I. N. 2007, *AJ*, 133, 2258
- Skrutskie, M. F., et al. 2006, *AJ*, 131, 1163
- Tsuji, T. 2005, *ApJ*, 621, 1033
- Warren, S. J., et al. 2007, *MNRAS*, 381, 1400
- West, A. A., et al. 2004, *AJ*, 128, 426
- Wilking, B. A., McCaughrean, M. J., Burton, M. G., Giblin, T., Rayner, J. T., & Zinnecker, H. 1997, *AJ*, 114, 2029
- York, D. G., et al. 2000, *AJ*, 120, 1579
- Young, E. T., et al. 2004, *ApJS*, 154, 428

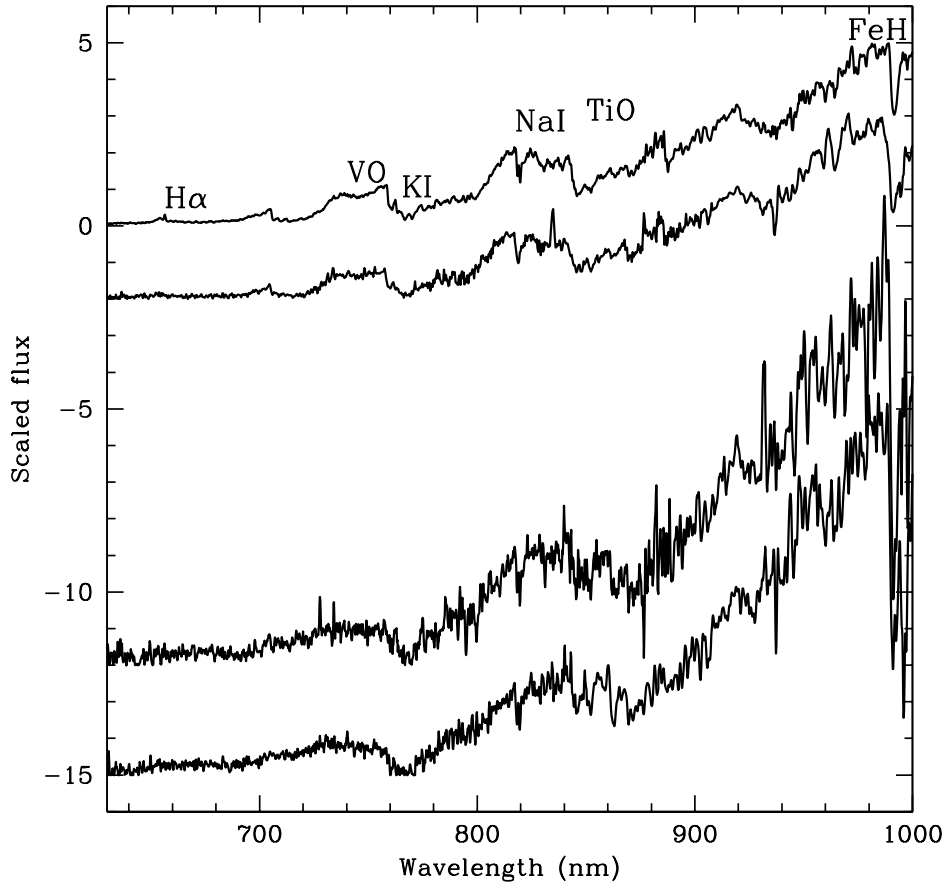


Fig. 1. Full spectra for 5 UD_s observed at SSO, including two of our objects with the latest spectral types. From top to bottom we show the spectra of VB10 (dM8), DENIS J1633131–755322 (dM9.5), DENIS J1206501–393725 (dL2), and DENIS J0014554–484417 (dL2.5). Some of the main spectral features discussed in this paper are labeled.

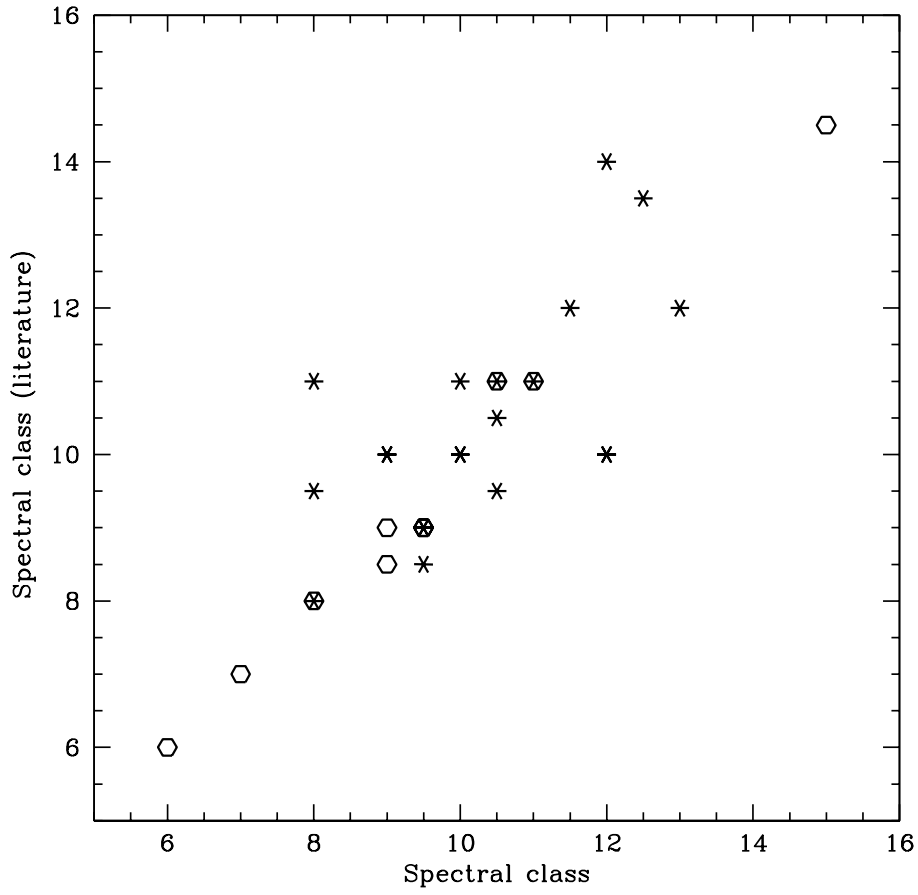


Fig. 2. Comparison between our spectral types and those in the literature. Open symbols denote the objects from the literature observed by us as spectral type references. Six pointed skeletal symbols denote DENIS UD candidates that have published spectral classification. Generally, there is a good agreement within the standard uncertainty associated with spectral type determination (± 0.5 subclass).

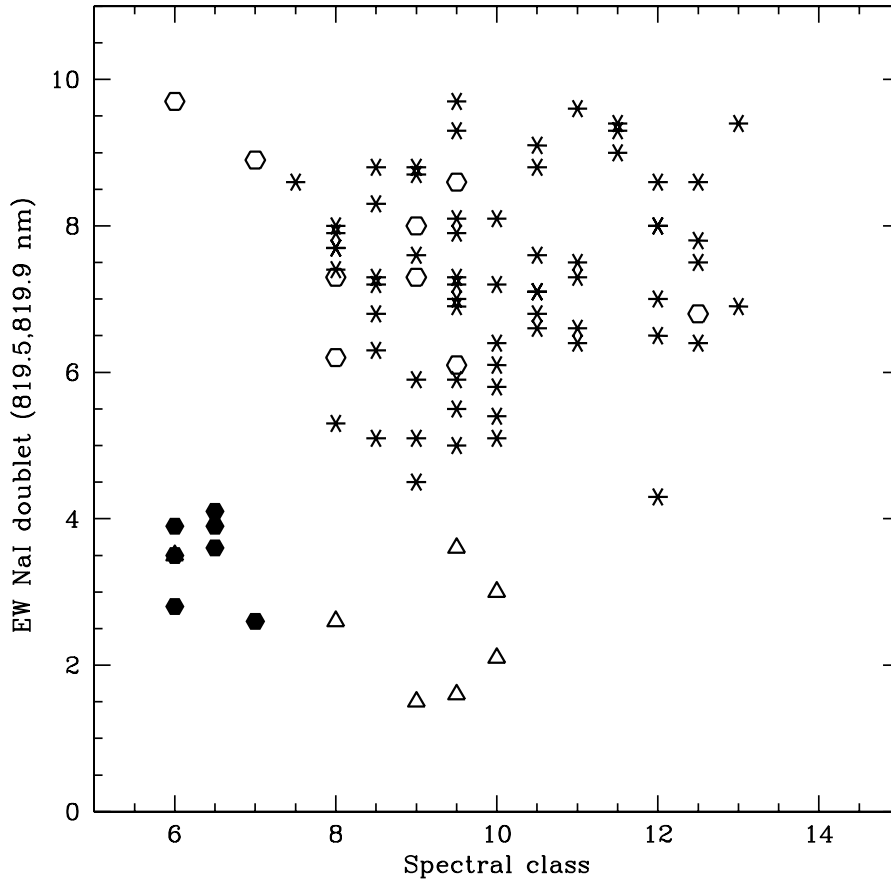


Fig. 3. Equivalent widths of the NaI doublet (given in Table 4) versus spectral type (listed in Table 3) for our 65 high-gravity program field objects (six pointed skeletal symbol), our 6 low-gravity program objects (open triangles), our 7 Upper Sco candidates (solid hexagons) and our 12 reference objects (open hexagons).

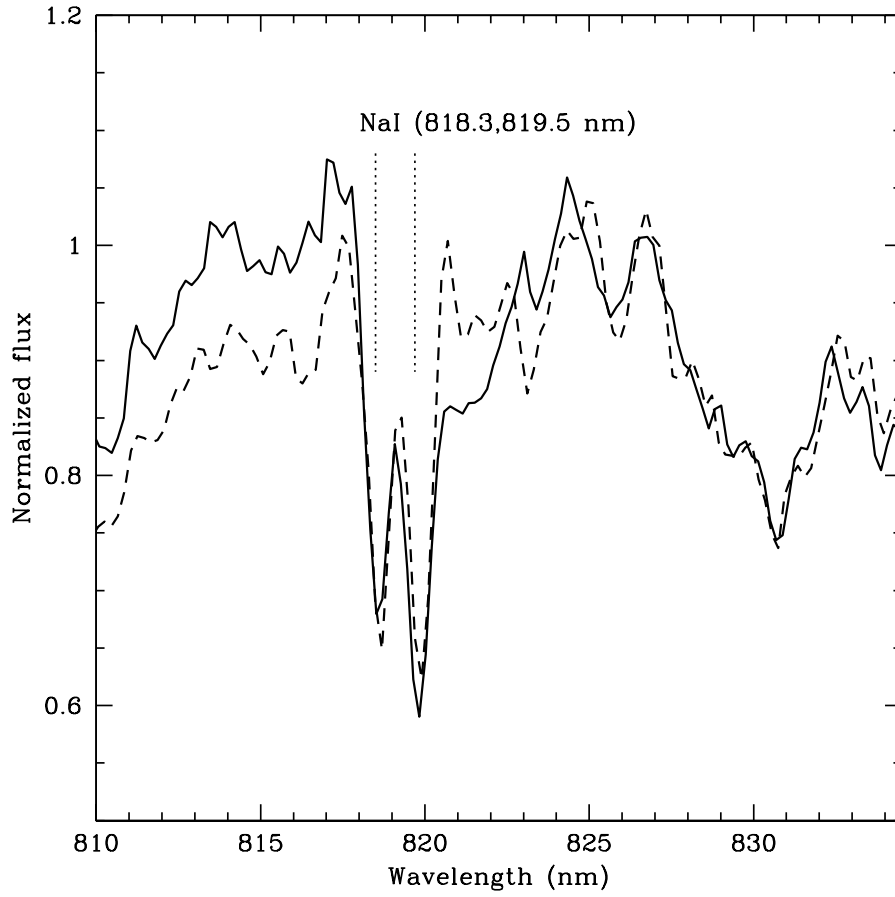


Fig. 4. Comparison of our two spectra of VB10 in the region around the NaI subordinate doublet. The solid line is the SSO spectrum (spectral resolution 8.5 \AA) and the dashed line is the CTIO spectrum (spectral resolution 7.5 \AA). The NaI doublet appears to be wider in the SSO spectrum because of blending effects with other absorption features.

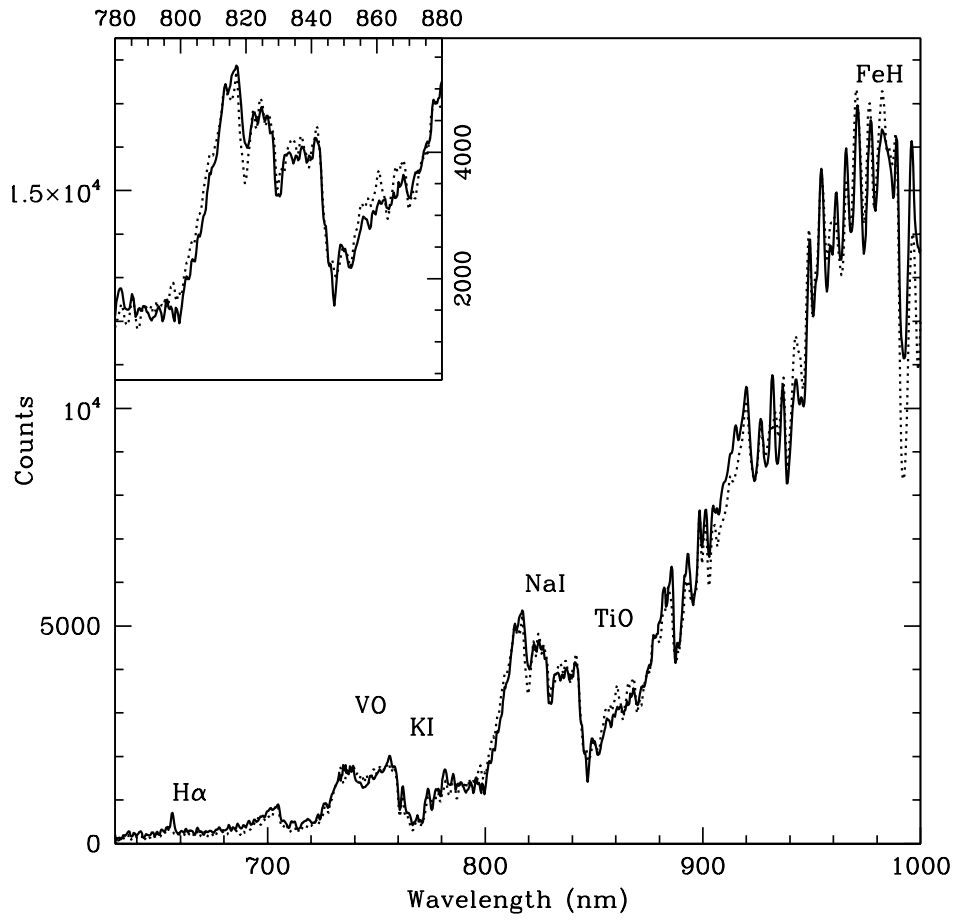


Fig. 5. Comparison of the SSO spectrum of DENIS J0006579-643654 (solid line) with the SSO spectrum of DENIS J2150133-661036 (dotted line) which was observed with the same instrumental setup and has the same spectral class (dL0). A zoom of the NaI spectral region is displayed in the upper left corner.

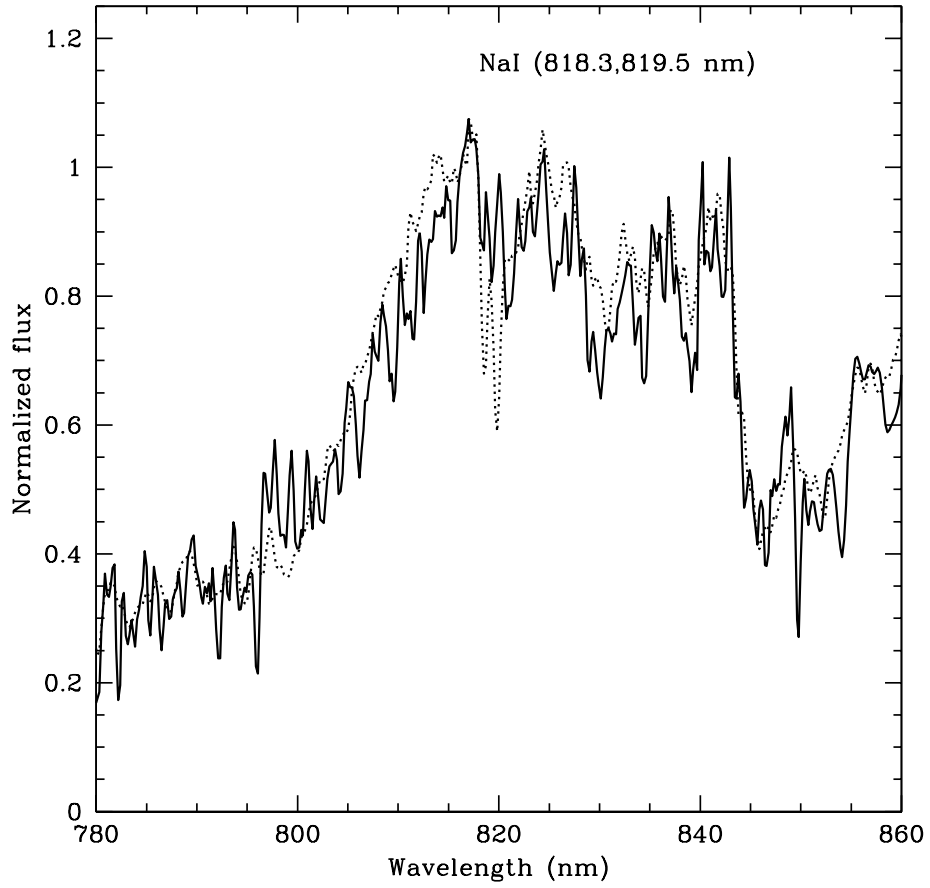


Fig. 6. Comparison of the SSO spectrum of DENIS J1901391–370017 (solid) with the spectrum of VB10 (dotted) obtained with the same instrumental setup. Both objects have the same spectral class (M8) but display different NaI subordinate doublet absorption.

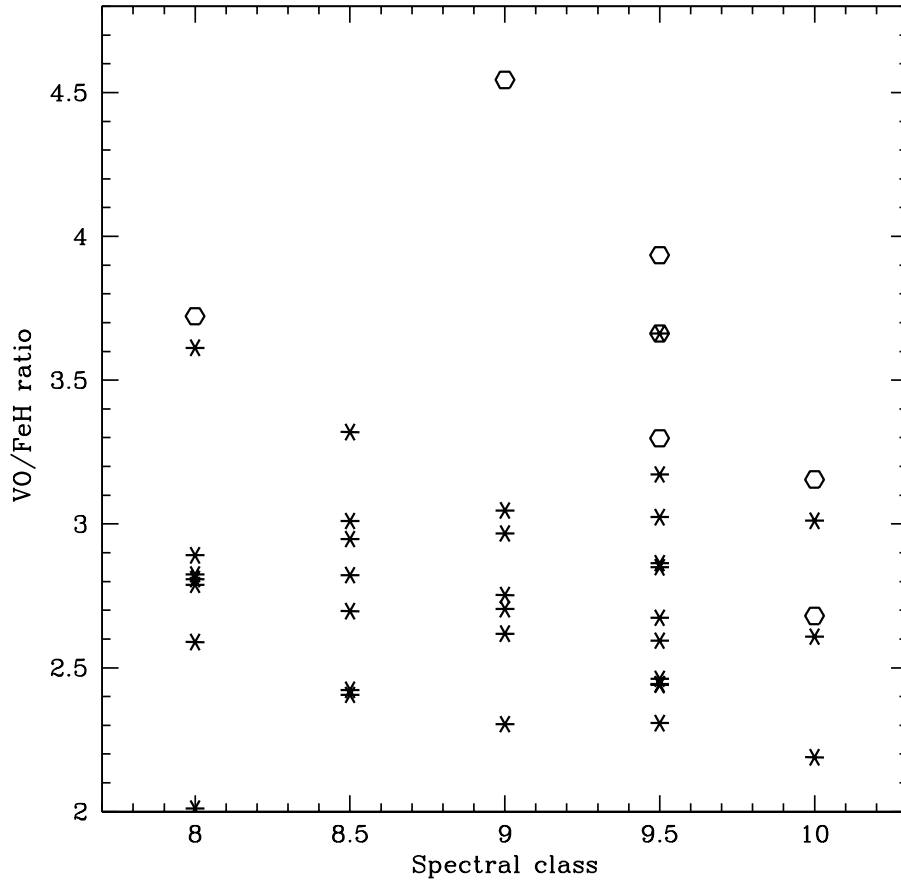


Fig. 7. Ratio of the VO versus FeH molecular band indices with respect to spectral subclass. The low-gravity objects are denoted with open hexagons and tend to display higher values than the rest of the sample.

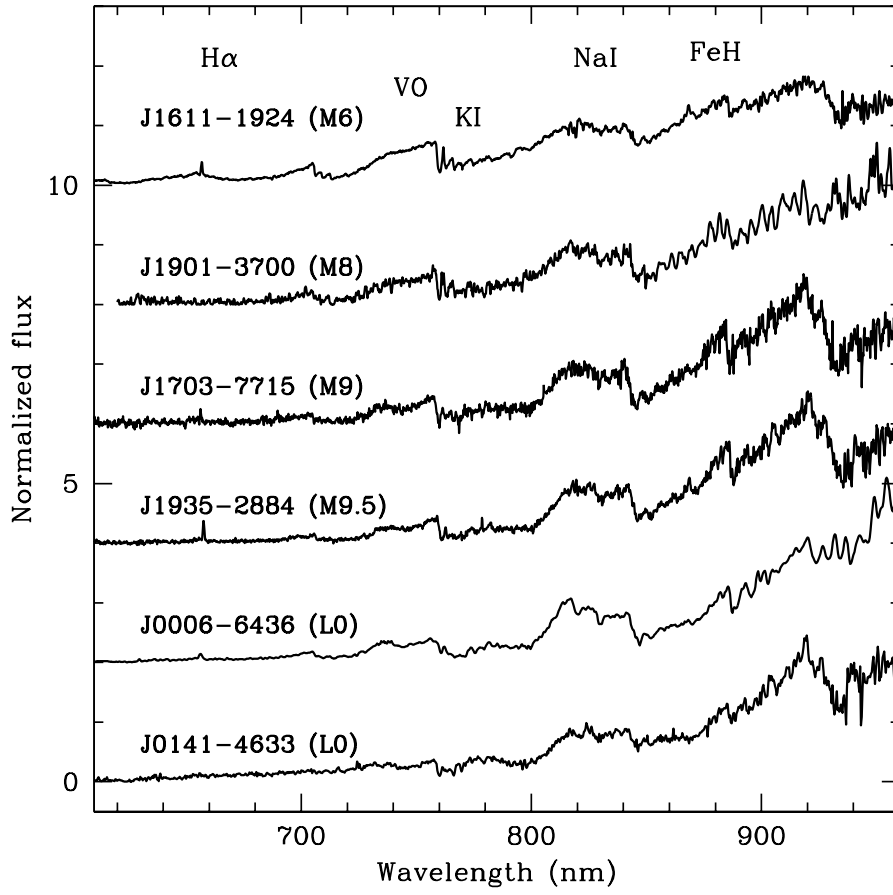


Fig. 8. Full spectra of five of our low-gravity UDs and one of our Upper Sco BDs.

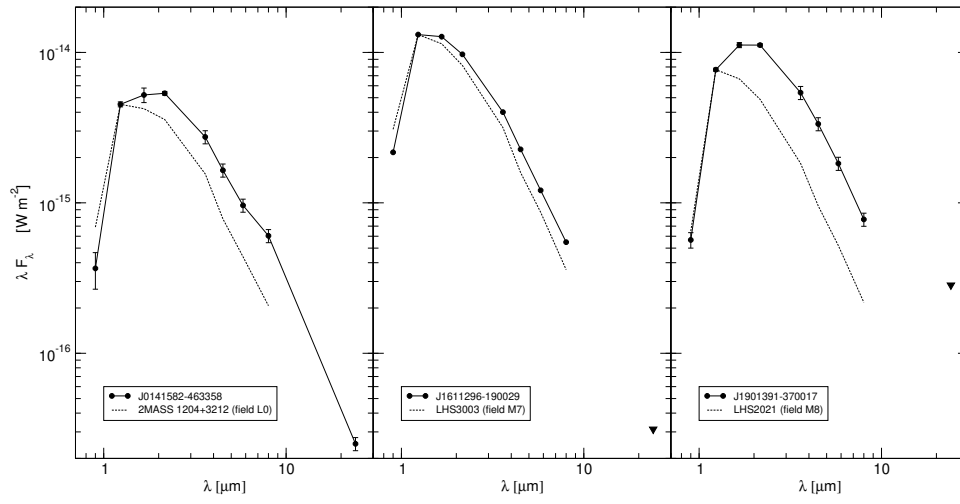


Fig. 9. Spectral energy distribution of our three young BDs that have been observed with Spitzer. Shown for comparison (dotted lines) are the spectral energy distributions of three normal dwarfs of similar spectral class.

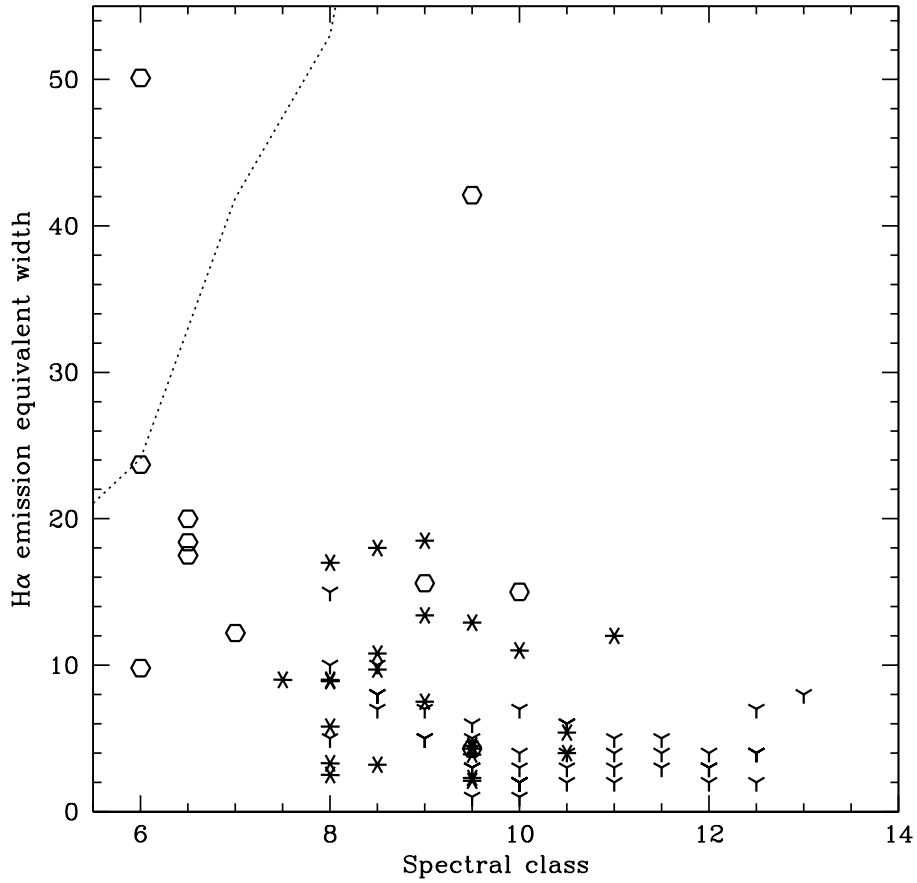


Fig. 10. $H\alpha$ equivalent width versus spectral class in our sample. Lower-gravity objects are denoted with open hexagons. Higher-gravity objects with $H\alpha$ detection are denoted with 6-pointed skeleton symbols. Objects for which $H\alpha$ was not detected in our spectra are shown as 3-pointed skeletons (upper limits). The dotted line is the boundary between accretors and non-accretors defined by Barrado y Navascués & Martín (2003).

Table 1. Photometric data for 78 DENIS ultracool dwarf candidates

DENIS name (1)	RA (J2000) (2)	Dec (J2000) (3)	<i>I</i> (4)	<i>I</i> − <i>J</i> (5)	<i>J</i> − <i>K</i> (6)	errI (7)	errJ (8)	errK (9)
J0000286−124514	00 00 28.7	−12 45 14	16.16	3.09	1.05	0.08	0.11	0.11
J0006579−643654	00 06 57.9	−64 36 54	16.71	3.28	1.32	0.12	0.09	0.11
J0014554−484417	00 14 55.4	−48 44 17	17.54	3.56	1.40	0.13	0.08	0.13
J0028554−192716	00 28 55.4	−19 27 16	17.61	3.66	1.18	0.18	0.18	0.17
J0031192−384035	00 31 19.3	−38 40 35	17.62	3.52	1.24	0.14	0.10	0.15
J0050244−153818	00 50 24.4	−15 38 18	16.86	3.20	1.10	0.10	0.10	0.11
J0053189−363110	00 53 19.0	−36 31 10	18.10	3.89	1.30	0.19	0.12	0.16
J0055005−545026	00 55 00.5	−54 50 26	17.12	3.38	1.00	0.11	0.20	0.15
J0116529−645557	01 16 52.9	−64 55 57	17.90	3.46	1.28	0.16	0.10	0.17
J0128266−554534	01 28 26.6	−55 45 34	17.07	3.26	1.47	0.16	0.12	0.13
J0141582−463358	01 41 58.2	−46 33 58	18.37	3.61	1.84	0.25	0.12	0.17
J0147327−495448	01 47 32.8	−49 54 48	16.05	3.14	0.97	0.07	0.09	0.07
J0206566−073519	02 06 56.7	−07 35 20	17.92	3.58	1.35	0.17	0.11	0.15
J0213371−134322	02 13 37.1	−13 43 22	17.64	3.36	1.03	0.17	0.16	0.18
J0224120−763320	02 24 12.0	−76 33 20	18.07	2.71	2.05	0.19	0.18	0.19
J0227102−162446	02 27 10.2	−16 24 46	17.04	3.37	1.49	0.11	0.12	0.18
J0230450−095305	02 30 45.0	−09 53 05	18.24	3.56	1.69	0.21	0.18	0.15
J0240121−530552	02 40 12.1	−53 05 52	18.18	3.83	1.36	0.22	0.10	0.16
J0301488−590302	03 01 48.8	−59 03 02	16.80	3.37	1.11	0.10	0.08	0.09
J0314352−462340	03 14 35.2	−46 23 41	17.99	3.13	1.15	0.20	0.15	0.20
J0325293−431229	03 25 29.4	−43 12 30	17.48	3.32	1.21	0.15	0.10	0.16
J0357290−441730	03 57 29.0	−44 17 31	17.91	3.39	1.73	0.19	0.16	0.17
J0427270−112713	04 27 27.1	−11 27 14	16.67	3.14	0.99	0.13	0.08	0.12
J0428510−225322	04 28 51.0	−22 53 22	16.80	3.35	1.48	0.10	0.08	0.11
J0436360−295947	04 36 36.0	−29 59 47	18.14	3.33	1.31	0.23	0.14	0.21
J0443376+000205	04 43 37.6	+00 02 05	15.88	3.35	1.42	0.05	0.10	0.11
J0529572−200300	05 29 57.2	−20 03 00	17.84	3.39	1.06	0.25	0.15	0.20
J0608528−275358	06 08 52.8	−27 53 58	17.09	3.41	1.47	0.10	0.09	0.11
J0610008−472741	06 10 00.9	−47 27 41	17.46	3.00	1.29	0.15	0.13	0.17
J0620165−430009	06 20 16.5	−43 00 09	17.78	2.82		0.18	0.13	
J0719317−505141	07 19 31.8	−50 51 41	17.44	3.44	1.09	0.11	0.09	0.14
J0921141−210445	09 21 14.1	−21 04 45	16.50	3.65	1.02	0.09	0.08	0.10
J0953213−101420	09 53 21.3	−10 14 20	16.82	3.30	1.41	0.10	0.08	0.11
J1004283−114648	10 04 28.3	−11 46 48	18.02	3.17		0.20	0.15	
J1004403−131818	10 04 40.3	−13 18 19	17.80	3.14	1.49	0.18	0.24	0.15
J1019245−270717	10 19 24.6	−27 07 17	16.90	3.33	1.08	0.10	0.08	0.15
J1115297−242934	11 15 29.7	−24 29 35	16.50	3.12	0.93	0.08	0.07	0.15
J1206501−393725	12 06 50.1	−39 37 26	17.67	3.36	1.19	0.16	0.10	0.16
J1216121−125731	12 16 12.1	−12 57 31	18.30	3.18		0.23	0.26	
J1232183−095149	12 32 18.3	−09 51 50	16.97	3.20	1.34	0.10	0.12	0.12
J1234018−112407	12 34 01.9	−11 24 07	18.22	3.59	1.23	0.19	0.13	0.20
J1256569+014616	12 56 56.9	+01 46 17	18.20	3.77	1.49	0.17	0.09	0.13
J1359551−403456	13 59 55.1	−40 34 56	16.98	3.20	1.16	0.10	0.10	0.13
J1411051−791536	14 11 05.2	−79 15 36	16.23	3.10	1.06	0.07	0.08	0.10
J1555256−181748	15 55 25.6	−18 17 48	14.75	2.35	1.09	0.05	0.10	0.10
J1600256−192750	16 00 25.6	−19 27 50	14.68	2.42	1.11	0.05	0.10	0.10
J1602043−205043	16 02 04.3	−20 50 43	15.16	2.40	0.94	0.05	0.10	0.10
J1602553−192243	16 02 55.3	−19 22 43	15.07	2.40	0.98	0.05	0.10	0.10
J1611014−192449	16 11 01.4	−19 24 49	15.69	2.41	0.91	0.05	0.10	0.10
J1611124−192737	16 11 12.4	−19 27 37	15.20	2.41	1.11	0.05	0.10	0.10
J1611296−190029	16 11 29.6	−19 00 29	16.46	2.80	1.19	0.05	0.10	0.10
J1622326−120719	16 22 32.7	−12 07 19	16.56	3.20	0.89	0.07	0.08	0.13
J1633131−755322	16 33 13.1	−75 53 23	16.20	3.10	1.10	0.06	0.07	0.10
J1703356−771520	17 03 35.6	−77 15 20	18.25	3.09		0.15	0.10	
J1707252−013809	17 07 25.2	−01 38 09	17.81	3.55	1.40	0.15	0.12	0.14
J1716352−031542	17 16 35.2	−03 15 42	14.46	3.43	1.71	0.05	0.10	0.09
J1753452−655955	17 53 45.2	−65 59 55	17.80	3.59	1.79	0.14	0.10	0.12

Table 1. continued.

DENIS name (1)	RA (J2000) (2)	Dec (J2000) (3)	<i>I</i> (4)	<i>I</i> − <i>J</i> (5)	<i>J</i> − <i>K</i> (6)	errI (7)	errJ (8)	errK (9)
J1901391−370017	19 01 39.1	−37 00 17	17.94	3.71	1.94	0.16	0.11	0.10
J1907440−282420	19 07 44.0	−28 24 20	17.95	3.60	0.97	0.16	0.12	0.18
J1926005−650006	19 26 00.5	−65 00 06	17.90	3.35	1.51	0.15	0.12	0.18
J1934511−184134	19 34 51.2	−18 41 35	17.71	3.43	1.15	0.14	0.11	0.16
J1935560−284634	19 35 56.0	−28 46 34	17.21	3.30	1.23	0.14	0.11	0.16
J1956460−774717	19 56 46.0	−77 47 17	17.46	3.28	1.14	0.13	0.11	0.18
J2013108−124244	20 13 10.8	−12 42 45	18.07	3.55	1.21	0.17	0.15	0.17
J2030412−363509	20 30 41.2	−36 35 09	17.50	3.19	1.21	0.16	0.09	0.12
J2045024−633206	20 45 02.4	−63 32 06	16.05	3.40	1.45	0.13	0.12	0.15
J2126340−314322	21 26 34.0	−31 43 22	16.26	3.06	0.91	0.07	0.13	0.16
J2139136−352950	21 39 13.6	−35 29 51	17.94	3.47	1.11	0.17	0.11	0.20
J2143510−833712	21 43 51.0	−83 37 12	16.50	3.30	0.98	0.10	0.06	0.11
J2150133−661036	21 50 13.3	−66 10 37	17.23	3.55	1.13	0.14	0.08	0.12
J2150149−752035	21 50 15.0	−75 20 36	17.45	3.51	1.39	0.16	0.09	0.12
J2243169−593219	22 43 17.0	−59 32 20	17.40	3.32	1.11	0.15	0.10	0.14
J2308113−272200	23 08 11.3	−27 22 01	18.11	3.53	1.40	0.20	0.17	0.17
J2322468−313323	23 22 46.8	−31 33 23	16.84	3.29	1.26	0.15	0.13	0.17
J2329343−540858	23 29 34.3	−54 08 58	18.37	3.41	1.74	0.20	0.12	0.21
J2330226−034717	23 30 22.6	−03 47 17	17.74	3.33	1.28	0.10	0.15	0.20
J2345390+005514	23 45 39.0	+00 55 14	16.90	3.18	1.28	0.12	0.13	0.13
J2354599−185221	23 54 59.9	−18 52 21	17.43	3.21	1.39	0.11	0.09	0.13

Table 2. Spectroscopic observing log

Name (1)	Telescope (2)	Date (3)	Texp (4)	Disp. (5)	Res. (6)
DENIS J0000286–124514	SSO 2.3m	23 June 2006	900	3.70	12.5
DENIS J0006579–643654	SSO 2.3m	23 June 2006	900	3.70	12.5
DENIS J0014554–484417	SSO 2.3m	27 June 2006	1200	1.87	8.5
DENIS J0028554–192716	SSO 2.3m	27 June 2006	1200	1.87	8.5
DENIS J0031192–384035	SSO 2.3m	27 June 2006	1200	1.87	8.5
	NTT	30 Dec 2000	2700	2.73	10.5
DENIS J0050244–153818	SSO 2.3m	27 June 2006	1200	1.87	8.5
	NTT	30 Dec 2000	1800	2.73	10.5
DENIS J0053189–363110	SSO 2.3m	28 June 2006	1200	1.87	8.5
DENIS J0055005–545026	SSO 2.3m	27 June 2006	1200	1.87	8.5
DENIS J0116529–645557	SSO 2.3m	27 June 2006	1200	1.87	8.5
DENIS J0128266–554534	SSO 2.3m	24 June 2006	1200	1.87	8.5
DENIS J0141582–463358	NTT	29 Nov 2003	2400	3.62	8.5
DENIS J0147327–495448	SSO 2.3m	24 June 2006	600	1.87	8.5
DENIS J0206566–073519	SSO 2.3m	27 June 2006	1200	1.87	8.5
DENIS J0213371–134322	SSO 2.3m	27 June 2006	1200	1.87	8.5
DENIS J0224120–763320	NTT	30 Dec 2000	2700	2.73	10.5
DENIS J0227102–162446	SSO 2.3m	27 June 2006	900	1.87	8.5
DENIS J0230450–095305	SSO 2.3m	28 June 2006	1200	1.87	8.5
DENIS J0240121–530552	SSO 2.3m	28 June 2006	1200	1.87	8.5
DENIS J0301488–590302	SSO 2.3m	27 June 2006	1200	1.87	8.5
DENIS J0314352–462341	VLT	12 Aug 2002	500	1.31	3.3
DENIS J0325293–431229	SSO 2.3m	24 June 2006	1700	1.87	8.5
DENIS J0357290–441731	VLT	12 Aug 2002	500	1.31	3.3
DENIS J0427271–112713	WHT	5 Dec 2006	1200	1.63	6.5
DENIS J0428510–225322	NTT	29 Nov 2003	2000	3.62	8.5
DENIS J0436360–295947	NTT	30 Dec 2000	2700	2.73	10.5
DENIS J0443373+000205	NTT	30 Dec 2000	900	2.73	10.5
DENIS J0529572–200300	NOT	9 March 2000	4800	3.10	20.0
	WHT	29 Sept 2000	900	2.90	6.5
DENIS J0608528–275358	WHT	28 Sept 2000	1200	2.90	6.5
DENIS J0610008–472741	NTT	30 Dec 2000	1800	2.73	10.5
DENIS J0620165–430010	NTT	30 Dec 2000	2700	2.73	10.5
DENIS J0719317–505141	SSO 2.3m	24 June 2006	900	3.70	12.5
DENIS J0921141–210445	SSO 2.3m	24 June 2006	600	3.70	12.5
DENIS J0953213–101420	NTT	30 Nov 2003	1500	3.62	8.5
DENIS J1004283–114648	NOT	9 March 2000	4800	3.10	20.0
	VLT	31 Dec 2002	1600	0.73	2.1
DENIS J1004403–131818	NOT	10 March 2000	2400	3.10	20.0
DENIS J1019245–270717	SSO 2.3m	24 June 2006	600	3.70	12.5
DENIS J1115297–242934	SSO 2.3m	22 June 2006	900	3.70	12.5
DENIS J1206501–393725	SSO 2.3m	25 June 2006	1200	1.87	8.5
DENIS J1216121–125731	NOT	10 March 2000	5400	3.10	20.0
DENIS J1232183–095149	NOT	10 March 2000	2260	3.10	20.0
DENIS J1234018–112407	SSO 2.3m	29 June 2006	1200	1.87	8.5
DENIS J1256569+014616	SSO 2.3m	29 June 2006	1200	1.87	8.5
DENIS J1359551–403456	SSO 2.3m	24 June 2006	1200	1.87	8.5
DENIS J1411051–791536	SSO 2.3m	22 June 2006	900	3.70	12.5
DENIS J1555256–181748	CTIO 4m	17 July 2007	1200	2.01	7.5
DENIS J1600256–192750	CTIO 4m	17 July 2007	1600	2.01	7.5
DENIS J1602043–205043	CTIO 4m	17 July 2007	1600	2.01	7.5
DENIS J1602553–192243	CTIO 4m	17 July 2007	1200	2.01	7.5
DENIS J1611014–192449	CTIO 4m	17 July 2007	1600	2.01	7.5
DENIS J1611124–192737	CTIO 4m	17 July 2007	1600	2.01	7.5
DENIS J1611296–190029	CTIO 4m	17 July 2007	2000	2.01	7.5
DENIS J1622326–120719	SSO 2.3m	24 June 2006	900	3.70	12.5
DENIS J1633131–755322	SSO 2.3m	22 June 2006	1200	3.70	12.5
DENIS J1703356–771520	CTIO 4m	17 July 2007	1600	2.01	7.5
DENIS J1707252–013809	SSO 2.3m	26 June 2006	1200	1.87	8.5
DENIS J1716352–031542	SSO 2.3m	22 June 2006	600	3.70	12.5
DENIS J1753452–655955	SSO 2.3m	26 June 2006	1200	1.87	8.5

Table 2. continued.

Name (1)	Telescope (2)	Date (3)	Texp (4)	Disp. (5)	Res. (6)
DENIS J1901391–370017	SSO 2.3m	27 June 2006	1800	1.87	8.5
DENIS J1907440–282420	SSO 2.3m	27 June 2006	1800	1.87	8.5
DENIS J1926005–650006	CTIO 4m	17 July 2007	1600	2.01	7.5
DENIS J1934511–184134	SSO 2.3m	25 June 2006	1200	1.87	8.5
DENIS J1935560–284634	CTIO 4m	17 July 2007	1600	2.01	7.5
DENIS J1956460–774717	CTIO 4m	17 July 2007	1600	2.01	7.5
DENIS J2013108–124244	SSO 2.3m	28 June 2006	1800	1.87	8.5
DENIS J2030412–363509	CTIO 4m	17 July 2007	1600	2.01	7.5
DENIS J2045024–633206	NTT	29 Nov 2003	600	3.62	8.5
DENIS J2126340–314322	SSO 2.3m	22 June 2006	1200	3.70	12.5
DENIS J2139136–352950	SSO 2.3m	25 June 2006	1200	1.87	8.5
DENIS J2143510–833712	SSO 2.3m	25 June 2006	1200	3.70	12.5
DENIS J2150133–661036	SSO 2.3m	23 June 2006	1200	3.70	12.5
DENIS J2150149–752035	SSO 2.3m	23 June 2006	1200	3.70	12.5
DENIS J2243169–593219	SSO 2.3m	23 June 2006	1200	3.70	12.5
DENIS J2308113–272200	SSO 2.3m	28 June 2006	1200	1.87	8.5
DENIS J2322468–313323	WHT	29 Sept 2000	1800	2.90	6.5
DENIS J2329343–540854	VLT	18 July 2002	500	1.31	3.3
DENIS J2330226–034717	WHT	29 Sept 2000	1800	2.90	6.5
DENIS J2345390+005514	SSO 2.3m	25 June 2006	1200	1.87	8.5
DENIS J2354599–185221	WHT	29 Sept 2000	1800	2.90	6.5
GJ 406	WHT	5 Dec 2006	300	1.63	6.5
LHS 2397a	SSO 2.3m	25 June 2006	400	1.87	8.5
LHS 2924	SSO 2.3m	26 June 2006	900	1.87	8.5
LP 944-20	WHT	28 Sept 2000	300	2.90	6.5
VB 8	SSO 2.3m	25 June 2006	360	1.87	8.5
VB 10	SSO 2.3m	25 June 2006	600	1.87	8.5
	CTIO 4m	17 July 2007	300	2.01	7.5
DENIS J1048147–395606	NTT	30 Nov 2003	60	3.62	8.5
DENIS J1228152–154733	VLT	17 June 2002	500	1.31	3.3
DENIS J1441373–094559	NOT	10 March 2000	4800	3.10	20.0
2MASS 003615+182112	WHT	28 Sept 2000	300	2.90	6.5

Table 3. PC3 index and spectral type for DENIS ultracool candidates

DENIS or name (1)	PC3 (2)	SpT (3)	Notes (4)
J0000286–124514	2.35	dM9.5	M8.5 (1)
J0006579–643654	2.42	dL0	low-gravity
J0014554–484417	3.64	dL2.5	
J0028554–192716	2.77	dL0.5	
J0031192–384035	3.70 ¹	dL2.5	
J0050244–153818	2.65 ²	dL0.5	L1: (1)
J0053189–363110	4.03	dL2.5	L3.5 (2)
J0055005–545026	1.94	dM8.5	
J0116529–645557	2.93	dL1	
J0128266–554534	2.84	dL1	L1 (3)
J0141582–463358	2.57	L0	L0 (4); low-gravity
J0147327–495448	1.80	dM8	M8+L2 (5)
J0206566–073519	1.98	dM8.5	
J0213371–134322	2.10	dM9	
J0224120–763320	2.55	dL0	
J0227102–162446	2.44	dL0	L1 (6)
J0230450–095305	2.40	dL0	
J0240121–530552	2.22	dM9.5	
J0301488–590302	2.11	dM9	L0 (7)
J0314352–462341	3.58	dL2	L0 (7)
J0325293–431229	2.05	dM8.5	
J0357290–441731	3.33	dL2	L0 (2); M9+L1.5 (8)
J0427271–112713	1.64	dM7	
J0428510–225322	2.78	dL0.5	L0.5 (9)
J0436360–295947	1.86	dM8	
J0443373+000205	2.25	dM9.5	M9 (10); low-gravity
J0529572–200300	2.10 ³	dM9.0	
J0608528–275358	2.21	dM9.5	low-gravity
J0610008–472741	2.01	dM8.5	
J0620165–430010	1.75	dM8	
J0719317–505141	2.87	dL1	
J0921141–210445	4.54	dL3	L2 (6)
J0953213–101420	2.45	dL0	L0 (1)
J1004283–114648	1.89	dM8	M9.5+L0.5 (8)
J1004403–131818	2.35	dL0	
J1019245–270717	2.74	dL0.5	M9.5 (3)
J1115297–242934	1.87	dM8	
J1206501–393725	3.15	dL2	
J1216121–125731	1.76	dM8	L1 (7)
J1232209–095102	0.97	M2	giant
J1234018–112407	2.36	dM9.5	
J1256569+014616	2.98	dL1.5	L2 (6)
J1359551–403456	3.08	dL2	
J1411051–791536	2.02	dM8.5	
J1555256–181748	1.48	M6	low-gravity
J1600256–192750	1.52	M6.5	low-gravity
J1602043–205043	1.50	M6.5	low-gravity
J1602553–192243	1.51	M6.5	low-gravity
J1611014–192449	1.41	M6	low-gravity
J1611124–192737	1.45	M6	low-gravity
J1611296–190029	1.61	M7	low-gravity
J1622326–120719	2.24	dM9.5	
J1633131–755322	2.28	dM9.5	
J1703356–771520	2.16	M9	low-gravity
J1707252–013809	2.82	dL0.5	
J1716352–031542	1.26	M5	giant
J1753452–655955	3.47	dL2	L4 (6)

Column 1: DENIS name. Column 2: PC3 index defined in M99. Column 3: Spectral type from PC3-SpT relation in M99. Column 4: Notes about specific targets found in the literature. References: (1)=Cruz et al. 2007; (2)=Kirkpatrick et al., in preparation (DwarfArchives.org); (3)=Kendall et al. 2007; (4)=Kirkpatrick et al. 2006; (5)=Reid et al. 2006; (6)=Schmidt et al. 2007; (7)=Bouy et al. 2003; (8)=Martín et al. 2006; (9)=Kendall et al. 2003; (10)=Hawley et al. 2002; (11)=Delfosse et al. 2001; (12)=Martín et al. 1999; (13)=Kirkpatrick et al. 2000 ¹ Average value of two independent measurements; PC3=3.75 (SSO) and PC3=3.65 (NTT) ² Average value of two independent measurements; PC3=2.80 (SSO) and PC3=2.50 (NTT) ³ Average value of two independent measurements; PC3=2.22 (SSO) and PC3=1.98 (NOT) ⁴ Average value of two independent measurements; PC3=1.86 (SSO) and PC3=1.97 (Blanco)

Table 3. continued.

DENIS or name (1)	PC3 (2)	SpT (3)	Notes (4)
J1901391–370017	1.81	M8	low-gravity
J1907440–282420	2.08	dM9	
J1926005–650006	2.04	dM9	
J1934511–184134	2.01	dM8.5	
J1935560–284634	2.33	dM9.5	low-gravity
J1956460–774717	2.35	dM9.5	
J2013108–124244	3.04	dL1.5	
J2030412–363509	1.83	dM8	
J2045024–633206	2.23	dM9.5	M9 (6)
J2126340–314322	2.32	dM9.5	
J2139136–352950	2.40	dL0	
J2143510–833712	2.21	dM9.5	
J2150133–661036	2.58	dL0	
J2150149–752035	2.91	dL1	
J2243169–593219	2.10	dM9	L0 (3)
J2308113–272200	2.97	dL1.5	
J2322468–313323	2.90	dL1	
J2329343–540854	4.26	dL3	
J2330226–034717	2.78	dL0.5	L1 (1)
J2345390+005514	2.10	dM9	
J2354599–185221	3.18	dL2	
GJ 406	1.52	dM6	dM6 (12)
LHS 2397a	2.13	dM9	dM8.5 (12)
LHS 2924	2.25	dM9.5	dM9 (12)
LP 944-20	2.12	dM9	
VB 8	1.65	dM7	dM7 (12)
VB 10	1.91 ⁴	dM8	dM8 (12)
DENIS 104814–395606	2.28	dM9.5	M9 (11)
DENIS 122815–154733	10.1	dL5	L4.5 (12)
DENIS 144137–094559	2.63	dL1	dL1 (12)
2MASS 003615+182112	3.71	dL2.5	L3.5 (13)

Table 4. Equivalent widths and molecular band indices

Name (1)	EW H α (2)	EW NaI(8170–8200) (3)	TiO (4)	VO (5)	CrH (6)	FeH (7)
DENIS J0000286–124514	-4.5 \pm -1	7.3 \pm 0.4	3.23	2.40	0.99	1.04
DENIS J0006579–643654	-15 \pm -2	3.0 \pm 0.4	3.61	2.65	0.92	0.84
DENIS J0014554–484417	>-4	8.6 \pm 0.8	2.29	2.06	1.47	1.53
DENIS J0028554–192716	-4 \pm -1	6.6 \pm 0.9	2.43	2.09	1.22	1.30
DENIS J0031192–384035 ¹	>-7	7.8 \pm 0.3	2.22	2.11	1.54	1.55
DENIS J0031192–384035 ²	>-2	7.5 \pm 0.4	2.12	2.26		
DENIS J0050244–153818 ¹	>-3	8.8 \pm 0.7	2.92	2.42	1.20	1.27
DENIS J0050244–153818 ²	>-4	7.6 \pm 1.2	2.87			
DENIS J0053189–363110	>-4	6.4 \pm 0.3	1.94	1.96	1.51	1.47
DENIS J0055005–545026	>-8	6.8 \pm 0.8	3.81	2.80	0.91	0.95
DENIS J0116529–645557	>-5	7.5 \pm 0.8	2.90	2.24	1.23	1.28
DENIS J0128266–554534	>-3	6.6 \pm 0.4	2.02	2.16	1.41	1.56
DENIS J0141582–463358	>-3	2.1 \pm 0.6	2.48	2.60	0.97	0.97
DENIS J0147327–495448	-17 \pm -1	7.4 \pm 0.9	3.88	2.64	0.97	0.94
DENIS J0205294–115925	>-3	5.2 \pm 0.2	1.81	1.68	1.44	1.23
DENIS J0206566–073519	-18 \pm -2	8.3 \pm 0.6	3.67	2.52	0.99	1.04
DENIS J0213371–134322	>-5	7.6 \pm 0.8	3.41	2.65	0.96	0.98
DENIS J0224120–763320	-11 \pm 4	6.1 \pm 0.9	2.63	2.27		
DENIS J0227102–162446	>-4	7.2 \pm 0.6	1.94	1.96	1.51	1.47
DENIS J0230450–095305	>-7	5.8 \pm 0.7	2.30	2.01	1.40	1.41
DENIS J0240121–530552	>-3	5.5 \pm 0.8	3.53	2.54	1.09	0.95
DENIS J0301488–590302	>-5	4.5 \pm 0.8	4.10	2.59	0.92	0.85
DENIS J0314352–462341	–	6.5 \pm 0.2	2.29	2.44	1.38	1.49
DENIS J0325293–431229	>-7	5.1 \pm 0.8	4.04	2.89	0.95	0.96
DENIS J0357290–441731	–	4.3 \pm 0.3	2.80	2.87	1.03	0.97
DENIS J0427271–112713	-9.0 \pm 1.2	8.6 \pm 0.8	4.16	2.53	0.98	0.99
DENIS J0428510–225322	-5.4 \pm 0.3	7.1 \pm 0.5	2.43	2.38	0.98	1.13
DENIS J0436360–295947	-8.9 \pm 0.8	7.7 \pm 0.5	4.29	2.66	0.98	0.92
DENIS J0443373+000205	-4.3 \pm 0.5	3.6 \pm 0.7	4.03	2.77	0.92	0.84
DENIS J0529572–200300 ³	-10.8 \pm 1.6	7.0 \pm 0.8	3.46	2.56	0.99	1.04
DENIS J0529572–200300 ⁴	-9.7 \pm 2.2	7.3 \pm 1.0	3.72	3.22	1.08	0.97
DENIS J0608528–275358	-3.9 \pm 0.5	5.0 \pm 0.7	3.97	2.93	0.94	0.80
DENIS J0610008–472741	-3.2 \pm 0.5	8.8 \pm 0.8	3.43	2.55	1.05	1.06
DENIS J0620165–430010	-9.0 \pm 0.3	7.7 \pm 0.5	3.03	2.74	0.98	0.97
DENIS J0719317–505141	-12:	9.6 \pm 0.8	2.42	2.50	0.64	1.02
DENIS J0921141–210445	>-8	9.4 \pm 0.8	2.25	2.03	1.21	1.34
DENIS J0953213–101420	>-2	5.4 \pm 0.9	3.24	2.68	0.96	0.89
DENIS J1004283–114648 ⁴	>-10	–	2.36	3.29	1.05	1.18
DENIS J1004283–114648 ⁵	-3.3 \pm 0.2	–	–	–	–	–
DENIS J1004403–131818	>-2	5.1 \pm 0.5	1.86	1.96	1.03	1.32
DENIS J1019245–270717	>-6	7.1 \pm 1.0	2.59	2.31	1.09	1.05
DENIS J1115297–242934	-5.8 \pm 0.7	7.9 \pm 0.4	3.94	2.46	0.94	0.95
DENIS J1206501–393725	>-4	8.6 \pm 0.8	2.26	2.08	1.38	1.43
DENIS J1216121–125731	>-5	8.0 \pm 0.7	3.78	1.85	1.11	0.92
DENIS J1234018–112407	>-6	8.1 \pm 0.9	2.71	2.65	0.98	0.93
DENIS J1256569+014616	>-5	9.0 \pm 0.3	1.97	2.17	1.36	1.46
DENIS J1359551–403456	>-3	9.6 \pm 0.4	2.45	2.32	1.19	1.34
DENIS J1411051–791536	>-8	6.3 \pm 0.8	4.05	2.54	0.99	0.90
DENIS J1555256–181748	-23.7 \pm 0.2	3.5 \pm 0.1	3.46	2.56	0.87	0.71
DENIS J1600256–192750	-18.4 \pm 0.2	3.6 \pm 0.1	3.41	2.56	0.87	0.72
DENIS J1602043–205043	-20.0 \pm 0.2	4.1 \pm 0.1	3.50	2.55	0.88	0.73
DENIS J1602553–192243	-17.5 \pm 0.2	3.9 \pm 0.1	3.41	2.56	0.88	0.74
DENIS J1611014–192449	-9.8 \pm 0.4	3.9 \pm 0.1	3.10	2.47	0.89	0.78
DENIS J1611124–192737	-50.1 \pm 0.8	2.8 \pm 0.1	3.33	2.51	0.87	0.76
DENIS J1611296–190029	-12.2 \pm 1.3	2.6 \pm 0.2	3.66	2.63	0.83	0.71
DENIS J1622326–120719	>-3	7.9 \pm 0.5	3.49	2.59	1.05	1.06
DENIS J1633131–755322	>-5	9.3 \pm 0.7	3.74	2.95	1.01	1.03
DENIS J1703356–771520	-15.6 \pm 2.4	1.5 \pm 0.6	4.43	3.09	0.81	0.68
DENIS J1707252–013809	>-6	9.1 \pm 1.1	2.42	2.22	1.45	1.48
DENIS J1716352–031542	-3.3 \pm 0.2	2.7 \pm 0.2	4.26	2.50	0.81	0.66
DENIS J1753452–655955	>-3	8.0 \pm 0.2	1.73	2.31	1.61	1.81

Column 2: H α equivalent width in Å. Column 3: NaI 818.3,819.5 nm doublet equivalent width in Å. Column 4: Sum of TiO indices defined in M99. Column 5: Sum of VO indices defined in M99. Column 6: CrH index defined in M99. Column 7: FeH index defined in M99. ¹ Measurements from SSO spectrum ² Measurements from NTT spectrum ³ Measurements from WHT spectrum ⁴ Measurements from NOT spectrum ⁵ Measurements from VLT spectrum ⁶ Measurements from CTIO Blanco spectrum

Table 4. continued.

Name (1)	EW H α (2)	EW NaI(8170–8200) (3)	TiO (4)	VO (5)	CrH (6)	FeH (7)
DENIS J1901391–370017	>-15	2.6±0.6	3.92	2.68	0.86	0.72
DENIS J1907440–282420	-18.5±0.6	8.7±0.8	3.99	2.56	0.94	0.93
DENIS J1926005–650006	-7.5±1.5	5.1±0.1	3.55	2.70	0.97	0.91
DENIS J1934511–184134	>-10	7.2±0.7	3.95	2.67	0.94	0.99
DENIS J1935560–284634	42.1±1.2	1.6±0.2	3.67	2.99	0.89	0.76
DENIS J1956460–774717	-4.3±1.0	7.2±0.1	3.76	2.66	1.06	1.09
DENIS J2013108–124244	>-3	9.3±0.6	2.46	2.19	1.21	1.40
DENIS J2030412–363509	-2.5±0.6	5.3±0.4	4.00	2.89	0.92	0.80
DENIS J2045024–633206	-2.3±0.5	5.9±0.6	3.54	2.76	0.95	0.87
DENIS J2126340–314322	-12.9±0.8	9.7±0.8	4.39	2.75	1.04	1.06
DENIS J2139136–352950	>-2	8.1±0.8	3.29	2.32	1.10	1.06
DENIS J2143510–833712	>-1	6.9±0.6	3.71	2.54	0.90	0.84
DENIS J2150133–661036	>-1	6.4±0.5	3.62	2.53	0.99	0.97
DENIS J2150149–752035	>-2	7.3±0.2	2.28	2.37	1.18	1.19
DENIS J2243169–593219	>-7	8.8±0.3	2.92	2.35	0.99	1.02
DENIS J2308113–272200	>-4	9.4±0.7	1.88	2.26	1.21	1.29
DENIS J2322468–313323	>-4	6.4±0.4	2.33	2.35	1.08	1.23
DENIS J2329343–540854	–	6.9±0.3	2.16	2.30	1.31	1.40
DENIS J2330226–034717	>-2	6.8±0.4	2.64	2.37	1.20	1.22
DENIS J2345390+005514	-13.4±0.7	5.9±0.6	3.87	2.54	0.99	0.97
DENIS J2354599–185221	>-2	7.0±0.4	2.21	2.27	1.26	1.48
GJ 406	-9.4±0.4	9.7±0.5				
LHS 2397a	-17.6±0.2	8.0±0.6	3.61	2.52	1.04	1.06
LHS 2924	-4.5±0.3	6.1±0.7	3.05	2.46	1.01	1.00
LP 944-20	-1.5±0.2	7.3±0.8	2.90	2.52	1.00	0.93
VB 8	-8.9±0.3	8.9±0.6	3.85	2.55	0.96	0.99
VB 10 ¹	-7.1±0.2	7.3±0.6	3.88	2.61	0.96	0.93
VB 10 ⁶	-8.8±0.1	6.2±0.3	4.01	2.71	0.95	0.91
DENIS J1048147–395606	-2.1±0.2	8.6±0.6	4.03	2.75	1.05	1.07
DENIS J1228152–154733	–	5.4±0.3	1.73	2.33	2.07	1.78
DENIS J1441373–094559	>-7	6±2	2.32	2.68	1.03	1.26
2MASS 003615+182112	>-2	6.8±0.3	2.01	2.18	1.74	1.66

Table 5. Absolute magnitudes and spectrophotometric distances for confirmed nearby dwarfs not known to be binaries

DENIS name (1)	SpT (2)	M_J (3)	Distance (pc) (4)	Distance error (5)
J0000286–124514	dM9.5	11.65	19.2	3.6
J0006579–643654	dL0	11.83	20.9	3.8
J0014554–484417	dL2.5	12.74	17.7	3.1
J0028554–192716	dL0.5	12.01	24.4	5.4
J0031192–384035	dL2.5	12.74	18.7	3.4
J0050244–153818	dL0.5	12.01	21.4	3.9
J0053189–363110	dL2.5	12.74	19.7	3.8
J0055005–545026	dM8.5	11.28	31.0	7.1
J0116529–645557	dL1	12.19	28.1	5.2
J0128266–554534	dL1	12.19	21.0	4.1
J0206566–073519	dM8.5	11.28	40.9	7.7
J0213371–134322	dM9	11.47	36.5	7.7
J0224120–763320	dL0	11.83	50.8	11.2
J0227102–162446	dL0	11.83	23.3	4.5
J0230450–095305	dL0	11.83	37.2	8.2
J0240121–530552	dM9.5	11.65	34.7	6.4
J0301488–590302	dM9	11.47	24.7	4.3
J0314352–462341	dL2	12.56	28.9	6.0
J0325293–431229	dM8.5	11.28	37.6	6.9
J0427271–112713	dM7	10.92	33.3	5.8
J0428510–225322	dL0.5	12.01	19.4	3.4
J0436360–295947	dM8	11.10	55.2	11.2
J0443373+000205	dM9.5	11.65	15.0	2.8
J0529572–200300	dM9	11.47	39.9	6.0
J0608528–275358	dM9.5	11.65	25.5	4.6
J0610008–472741	dM8.5	11.28	43.2	8.5
J0620165–430010	dM8	11.10	59.1	11.7
J0719317–505141	dL1	12.19	23.0	4.1
J0921141–210445	dL3	12.92	9.7	1.7
J0953213–101420	dL0	11.83	21.8	3.8
J1004283–114648	dM8	11.10	56.2	11.6
J1004403–131818	dL0	11.83	36.8	9.2
J1019245–270717	dL0.5	12.01	20.5	3.6
J1115297–242934	dM8	11.10	28.5	4.9
J1206501–393725	dL2	12.56	22.4	4.1
J1216121–125731	dM8	11.10	63.6	16.4
J1234018–112407	dM9.5	11.65	39.5	7.8
J1256569+014616	dL1.5	12.38	25.8	4.6
J1359551–403456	dL2	12.56	17.6	3.2
J1411051–791536	dM8.5	11.28	23.4	4.1
J1622326–120719	dM9.5	11.65	22.0	3.8
J1633131–755322	dM9.5	11.65	19.5	3.3
J1707252–013809	dL0.5	11.47	54.8	10.1
J1753452–655955	dL2	12.56	21.4	3.9

Column 1: DENIS name. Column 2: Spectral type adopted in this paper. Column 3: Absolute J-band magnitude estimated from the absolute magnitude vs. $I - J$ color relationship given in Phan-Bao et al (2008). Column 4: Spectrophotometric distance in parsecs.

Table 5. continued.

DENIS name (1)	SpT (2)	M_J (3)	Distance (pc) (4)	Distance error (5)
J1907440–282420	dM9	11.47	37.7	7.3
J1926005–650006	dM9	11.47	41.4	8.0
J1934511–184134	dM8.5	11.28	39.7	7.5
J1956460–774717	dM9.5	11.65	32.1	6.1
J2013108–124244	dL1.5	12.38	26.8	5.6
J2030412–363509	dM8	11.10	43.8	7.9
J2045024–633206	dM9.5	11.65	15.9	3.1
J2126340–314322	dM9.5	11.65	20.4	4.0
J2139136–352950	dL0	11.83	33.7	6.4
J2143510–833712	dM9.5	11.65	20.4	3.4
J2150133–661036	dL0	11.83	23.4	4.1
J2150149–752035	dL1	12.19	22.3	4.0
J2243169–593219	dM9	11.47	33.3	6.1
J2308113–272200	dL1.5	12.38	27.6	6.0
J2322468–313323	dL1	12.19	18.7	3.7
J2329343–540854	dL3	12.92	25.6	4.9
J2330226–034717	dL0.5	12.01	30.2	6.3
J2345390+005514	dM9	11.47	28.2	5.6
J2354599–185221	dL2	12.56	21.5	3.9

Table 6. *Spitzer* observation log

Object	Program ID	P.I.	Obs. Date	Instrument
J0141582-463358	30540	Houck	2006-08-12	IRAC1-4
J0141582-463358	284	Cruz	2007-07-16	MIPS1
J1611296-190029	20103	Hillenbrand	2005-08-24	IRAC1-4
J1611296-190029	20103	Hillenbrand	2006-04-06	MIPS1
J1901391-370017	6	Fazio	2004-04-20	IRAC1-4
J1901391-370017	6	Fazio	2004-04-11	MIPS1

Table 7. *Spitzer* mid-IR photometry

Object	3.6 μm [mJy]	4.5 μm [mJy]	5.8 μm [mJy]	8.0 μm [mJy]	24 μm [mJy]
J0141582-463358	3.29	2.47	1.86	1.61	0.20
J1611296-190029	4.81	3.40	2.34	1.46	<0.25
J1901391-370017	6.48	5.02	3.53	2.07	<2.27